DOI: http://dx.doi.org/10.32571/ijct.1410570 **E-ISSN: 2602-277X**

International Journal of Chemistry and Technology

http://dergipark.org.tr/ijct

Research Article

Investigation, Structural Characterization and Evaluation of the Biological Potency by Molecular Docking of Amoxicillin Analogue of a Schiff Base Molecule

Veysel TAHİROGLU[1*], Kenan GOREN[2], Ümit YİLDİKO[3], Mehmet BAGLAN[2]

[1]*Şırnak University, Faculty of Health Sciences, Department of Nursing, Şırnak, Turkey*

[2]*Kafkas University, Department of Chemistry, Kars Turkey*

[3]*Kafkas University, Department of Bioengineering, Kars Turkey*

Received: 27 December 2023; Revised: 13 September 2024; Accepted: 16 September 2024

*****Corresponding author veysel.tahiroglu@sirnak.edu.tr

Citation: Tahiroglu V; Goren, K.; Yildiko, U.; Baglan, M. *Int. J. Chem. Technol*. 2024, 8(2), 190-199.

ABSTRACT

We describe the Theoretical Chemical Calculations of the amoxicillin-based Schiff base generated by the interaction of the antibiotic amoxicillin with 2,6-diaminopyridine in this work. The Gaussian09 software program was used for this. Quantum chemical calculations of the compound (molecular geometry, geometric structure, optimized geometric parameters, bond angle and bond length) have been carried out using SDD and 6-311G basis sets and density functional theory (DFT/ B3LYP) and (DFT/B3PW91) tehniques. The HOMO-LUMO energies of our compound were determined utilizing the DFT method with two methods and basis sets. The compound's molecular electrostatic potential (MEP) surface, NBO analysis, Nonlinear Optical Properties (NLO), Mulliken atomic charges have been calculated using two methods and sets. In the last phase of this study, the compound was subjected to molecular docking studies for enzyme inhibition. Furthermore, homology modeling and molecular docking analysis have been done to assess the biological and medical aspects of this ligand by measuring the attraction intensity and attraction energies of molecular ligand-biological contact complexes.

Keywords: DFT, MEP, NBO. Amoxicillin, Schiff Base, 2,6−Diaminopyridine, Molecular Docking.

1. INTRODUCTION

Alzheimer's disease (AD) is a neurodegenerative brain disease that is characterized by amyloid b peptide (Ab) deposits (amyloid plaques) and oxidative stress byproducts.[1] Amyloid plaques are predominantly comprise of the 42 amino acid-long Ab isoform (Ab1e42), which forms cytotoxic structures ranging from monomers to oligomers (2e6 monomers) to fibers. In clinical studies for the treatment of Alzheimer's illness, a few small molecules [e.g., elenbecestat (E2609), umibecestat (CNP520)] and macromolecules (e.g., gantenerumab, CAD106, UB-311) that target the generation and clearance of Ab monomers, oligomers, and fibers are presently being studied.[2] Potential anti-Alzheimer medicines are compounds that can interact with single or several targets implicated in the etiology of Alzheimer's disease (AD). Cholinesterases [acetylcholinesterase (AChE) and butyrylcholinesterase (BChE)] were studied in order to create novel anti-Alzheimer medicines.[3] The cholinergic system is severely affected by neurodegeneration and synaptic dysfunction in Alzheimer's disease, resulting in a drop in levels of the neurotransmitter acetylcholine (ACh) that causes memory loss and cognitive impairment, a condition specific to Alzheimer's patients. Acetylcholinesterase (AChE) and butyrylcholinesterase (BChE) are two cholinesterases (ChE) that catalyze the hydrolysis of ACh to terminate cholinergic neurotransmission. Inhibiting ACh hydrolysis in the brains is utilized to boost ACh levels, restoring cognitive abilities and alleviating AD symptoms.[4] Many investigations on the *in-vitro* biological activities of Schiff base ligands for drug development have been published. Theoretical investigations are utilized to validate experimental results based on the biological activities of this ligand family. To rapidly and precisely

DOI: http://dx.doi.org/10.32571/ijct.1410570 E-ISSN: 2602-277X

anticipate and justify ligand activity, molecular docking has recently been widely employed to free energies, quantify ligand-receptor interaction, and inhibition constants of generated compounds depending on the empirical Screen Score function.[5]

Schiff bases are excellent nitrogen donor ligands (-C=N-). During the creation of the coordination complex, these ligands transfer one or more electron pairs to the metal ion. To generate very stable 4, 5, or 6 ring complexes, Schiff bases must have a second functional group with a replaceable hydrogen atom as near to the azomethine group as feasible.[6] This group should preferably be hydroxyl. Schiff base complexes In the preparation of some drugs, in the production of dyestuffs, in the electronics industry, plastics industry, agriculture, cosmetics and polymer production, analytical. They are substances of increasing importance in various branches such as chemistry and liquid crystal technology. In recent years, Schiff base complexes have been used in medicine due to their anticancer activity.[7] Its importance in the world is increasing and it is used as a reagent in the fight against cancer is being investigated. Despite the availability of several novel antibacterials in recent years, amoxicillin, either alone or in combination with clavulanic acid, remains one of the most extensively used antibacterial agents.[8] Although they are often considered 'twin drugs', they differ in both antibacterial activities and safety profiles. It is widely established that the clavulanate component alone can induce unpleasant responses, exposing patients to increased and, in some cases, excessive risks.[9]

Computer-aided quantum chemical calculations are performed using molecular modeling tools to help experimental research or to forecast the findings to be attained without completing experimental studies.[10] The primary goal of these programs is to develop efficient algorithms for calculating molecule attributes such as molecular structure, total energy, dipole moment, optimal geometry, and vibration wave numbers. Such computations are based on quantum mechanics. Quantum mechanical rules were first applied to atoms and molecules shortly after the establishment of quantum theory. In theory, quantum theory can compute all of a molecule's chemical characteristics. Many properties of molecules, such as bond length, bond angle, dipole moments mulliken atomic charges, and HOMO-LUMO energies, may be determined theoretically using computers.[11]

The DFT method is used to compute monomers, oligomers, and polymers. Density functional theory (DFT) is a popular tool for determining the electrical and geometric structure of molecules. Becke, threeparameter, Lee-Yang-Parr (B3LYP) technique with 6-311G (d,p) basis set in Gaussian 09 software was utilized for DFT experiments.[12]

2. MATERIALS AND METHODS

All calculations in this work, which supports the experimental data of the manufactured molecule, were performed using the Gaussian 09W package software, which includes several method and basis set possibilities. The molecule's geometric, electrical, spectroscopic, and thermodynamic properties were computed utilizing the SDD and 6-311G basis sets using DFT(B3LYP, B3PW91) techniques.[12] At this stage, the molecule must first achieve its lowest-energy, most stable three-dimensional configuration. The molecule was drawn in the "GaussView 6.0.16" software and optimized in the Gaussian 09W program using the technique and basis set we selected. This most steady structure served as the foundation for all computations. The major molecule's geometric characteristics (bond length, angle), electronegativity (χ), total energy, atomic charges, dipole moment (μ), chemical hardness (η) and softness (S), ionization potential (I), and energy difference (ΔEg). Features such as DFT(B3LYP, B3PW91) and SDD, 6-311G were calculated in two different basis sets. In determining the most stable conformations of molecules, the molecules are analyzed in the ChemDraw program. After drawing, the stable conformations were calculated by transferring them to the Marvin Beans program. Minimization of calculated stable conformations of molecules in Chem3D program has been made. Optimization of the minimized molecules in the Gaussian09 program again The most stable conformations were computed utilizing DFT(B3LYP, B3PW91) and SDD, 6-311G sets in the DFT technique. Using the same methods and sets, the geometry optimizations of the molecule, geometric parameters, minimum molecular energies, Mulliken charges, molecular electrostatic potential surfaces and boundary orbitals, and HOMO and LUMO energies have been calculated. E energy differences were computed for each approach using the estimated HOMO and LUMO energy values.

3. RESULTS and DISCUSSION

3 .1. Structure Details and Analysis

The geometry of a molecule is related to the bond lengths and bond angles between its atoms. It is also one of the most important factors that determine the physical and chemical characteristics of the molecule.[13] In the GaussView 6.0.16 molecular imaging program plotted, utilizing the Density Function Theory (DFT) method, with SDD VE 6-311G sets, which include polarizing functions added to eliminate the polarization effect and diffusing functions added to model the electron density being more dispersed in excited, ionic molecules compared to the ground condition of the component.[3] The space placement and space structure of the atoms in the molecule were determined by geometry optimization with restricted closed shell calculations in which they are forced to take part in an orbit. Thus, bond lengths (Å), bond angles (º) and dihedral angles (º) calculated

DOI: http://dx.doi.org/10.32571/ijct.1410570 E-ISSN: 2602-277X

theoretically.[14] Some bond angles and bond lengths of our molecule obtained with the two methods and sets used are given in Table 1. When we look at the bond lengths in Table 1, high deviations are observed in C4-C8 (1.53016 Å), C8-C10 (1.55568 Å), C13-C16 (1.58135 Å) atoms, while low deviations are observed in C10-O11 (1.25821 Å), C29-N31 (1.38040 Å) atoms. In trihedral structures, a large deviation of O23-C22-O24 with a bond angle of 121.79950° was determined. In tetrahedral structures, a large change in bond angle was observed between N9-C8-C10-O11 atoms.

Table 1. Theoretically obtained some bond lengths (Å) and bond angles (°) of the Schiff base compound.

Bond Lengths	B3LYP/SDD	B3PW91/6-311G	Bond Lengths	B3LYP/SDD	B3PW91/6-311G
C2-C3	1.40558	1.39279	C6-H36	1.08967	1.08486
C1-C6	1.41090	1.39667	C8-H38	1.11030	1.10614
C4-C8	1.53016	1.51827	C16-H43	1.09045	1.08544
C8-C10	1.55568	1.53856	C29-N31	1.38040	1.36577
C13-C16	1.58135	1.56505	C25-N32	1.41161	1.40147
C17-C22	1.52280	1.50602	C29-N31	1.38040	1.36577
C25-C26	1.40943	1.39596	C10-O11	1.25821	1.24870
C27-C28	1.40094	1.38768	C22-O24	1.37861	1.36333
C28-C29	1.42523	1.41163	C1-O7	1.40103	1.38881
C13-H42	1.09319	1.08920	C16-S19	1.89458	1.89382
Bond Angles	**B3LYP/SDD**	**B3PW91/6-311G**	**Bond Angles**	**B3LYP/SDD**	**B3PW91/6-311G**
C4-C5-C6	120.80627	120.74670	C21-C18-C20	111.11031	111.63533
C5-C4-C8	120.47666	120.39861	H45-C20-H46	108.51955	107.89703
C8-C10-N12	116.48672	116.88880	O23-C22-O24	121.79950	121.94129
C13-C14-N15	91.45076	91.24920	C16-S19-C18	92.86229	92.68122
C18-C17-C22	115.11704	115.20950	N31-C29-N30	116.34701	116.20031
Planar Bond Angles	**B3LYP/SDD**	**B3PW91/6-311G**	**Planar Bond Angles**	**B3LYP/SDD**	**B3PW91/6-311G**
C5-C4-C8-N9	-37.43537	-34.46955	C16-S19-C18-C17	-12.36380	-12.91661
N9-C8-C10-O11	-26.84206	-30.55301	C14-N32-C25-N30	-3.82094	-3.42030
N15-C14-N32-C25	-1.7076	-1.56354	N15-C17-C22-O24	-48.07146	-46.85910
C16-N15-C17-C18	-33.05986	-35.17496	C25-N30-C29-N31	-179.02932	-178.91379

3.2. Mulliken Atomic Charges

The values of Mulliken atomic charges of the molecule are given in Table 2. Reactive atomic charges play a significant part in quantum mechanical computations in molecular systems.[15] In this study, our molecule was calculated using DFT(B3LYP, B3PW91) methods and SDD, 6-311G sets. It has been observed that the electronegative atoms N12 (-0.379), N15 (-0.138), N30 (-0.137), N31(-0.673), O7 (-0.466), O11 (-0.315), O23 (-0.300) and O24 (-0.429) in the molecule have negative charge values. a) Structure Optimization, b) Mulliken Charge, c) Atomic Mass d) Bond Lengths obtained with the SDD basis set and B3LYP method are given in Figure 1.

Table 2. Mulliken atomic charges of the Schiff base compound.

ATOMS	B3LYP/ SDD	B3PW91/ 6-311G	ATOMS	B3LYP/ SDD	B3PW91/ 6-311G
C8	-0.267	-0.268	O23	-0.300	-0.418
C10	0.215	0.621	O24	-0.429	-0.549
C13	-0.108	-0.205	N9	-0.665	-0.757
C14	-0.022	0.502	N12	-0.379	-0.663
C16	-0.429	-0.204	N15	-0.138	-0.528
C17	-0.072	-0.133	N30	-0.137	-0.541
C18	-0.096	-0.447	N31	-0.673	-0.890
C20	-0.646	-0.518	N32	0.005	-0.379
C21	-0.625	-0.470	S19	0.188	0.263
C22	0.089	0.609	H39	0.319	0.338
C26	-0.378	-0.200	H40	0.266	0.301
C27	-0.124	-0.104	H41	0.344	0.379
C28	-0.342	-0.212	H42	0.299	0.277
C29	0.174	0.538	H43	0.283	0.250
O7	-0.466	-0.633	H45	0.215	0.212
O11	-0.315	-0.445	H46	0.206	0.210

DOI: http://dx.doi.org/10.32571/ijct.1410570 E-ISSN: 2602-277X

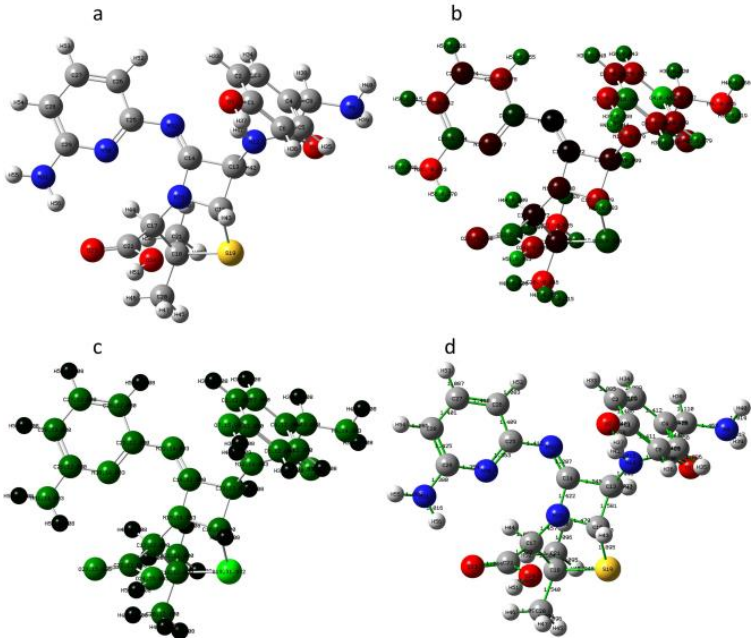

Figure 1. a) Structure Optimization, b) Mulliken Charge, c) Atomic Mass d) Bond Lengths of the the Schiff base compound with DFT/B3LYP/SDD basis set.

3.3. HOMO and LUMO Analysis

The most significant orbitals in a structure are the frontier molecular orbitals (FMO), the highest occupied molecular orbital (HOMO), and the lowest unoccupied molecular orbital (LUMO), all of ,which have a key role in the electrical and optical features of a molecule.[16] HOMO energy is related to the potential to donate electrons and LUMO energy is associated with the potential to gain electrons. The energy gap, or the difference in HOMO-LUMO energy levels, is a key quantity in defining the electrical characteristics of the molecule.[17] The energy gap also describes the chemical stability of the molecule and the charge transfer that occurs within the structure. Essentially, the energy gap determines the energy required to move from the most stable ground state within the molecule to an exciting state.[18] As shown in Figures 2 and 3, two fundamental molecular orbitals of our molecule were examined for the HOMO and LUMO energies obtained using the two methods and basis sets used. The quantum chemical parameters considered for the low energy conformations of the molecule employing the DFT/B3LYP/SDD and DFT/B3PW91/6-311G methods and basis sets are showed in Table 3. Energy between HOMO, LUMO and HOMO-LUMO gap (E_{GAP}) allows to describe the chemical behavior and reactivity of molecules. In reactions, the HOMO of the nucleophile reacts with the LUMO of the electrophile.[19] Whether the E_{GAP} value is numerically large or small determines the reaction mechanism and reaction conditions. Whether the E_{GAP} value is numerically large or small is important to predict the color of the molecule in the visible region. A numerically small E_{GAP} value indicates conjugation and causes excitation at lower energy. If the E_{GAP} value is numerically higher, the probability of conjugation is much less and causes stimulation at higher energy. Because molecules with low-energy E_{GAP} values can be excited by low energies, they often show some interesting optical properties.[20] They have electronic characteristics as well, such as intramolecular electron transport (in solution) and metallic conductivity (in solid state). The calculated E_{GAP} value of 4.3061 eV means that the compound is reactive in reactions, is a good ligand for metals, shows conductive properties, has conjugation and is a colored compound, and means that it is a candidate compound for these fields.

DOI: http://dx.doi.org/10.32571/ijct.1410570 E-ISSN: 2602-277X

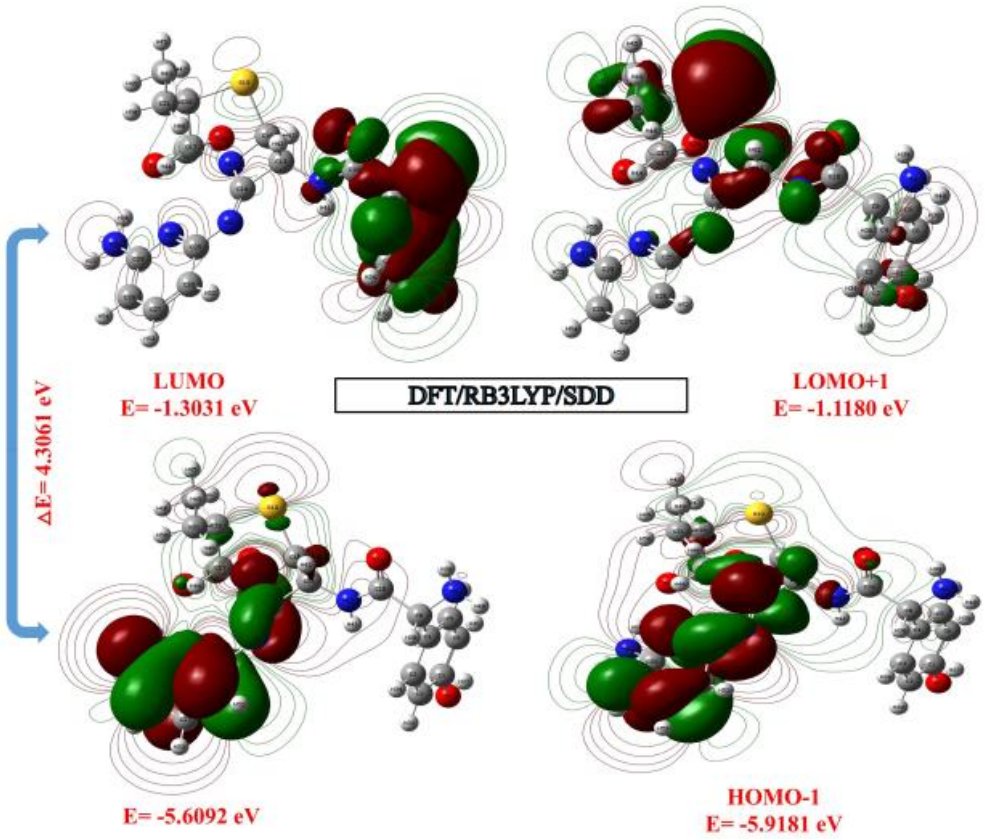

Figure 2. HOMO, LUMO values and band gap energies of the Schiff base compound obtained with the DFT/B3LYP/SDD method and basis set.

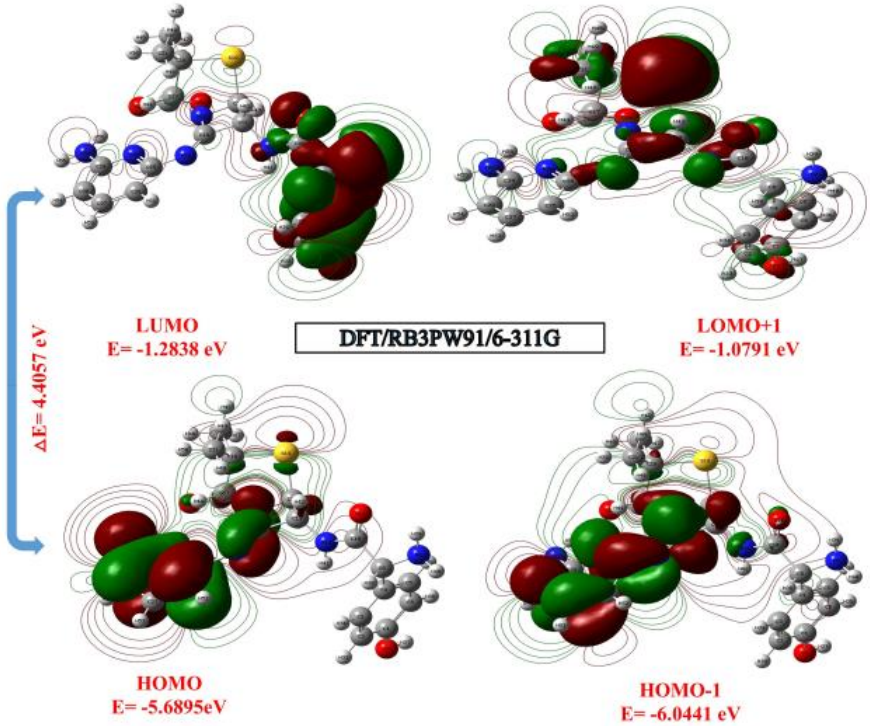

Figure 3. HOMO, LUMO values and band gap energies of the Schiff base compound obtained with the DFT/B3PW91/6-311G method and basis set.

DOI: http://dx.doi.org/10.32571/ijct.1410570 E-ISSN: 2602-277X

Table 3. Calculated quantum chemical parameters*(in eV) for low energy compatibilities by DFT/B3LYP/SDD-DFT/B3PW91/6-311G methods of the Schiff base compound.

Molecules Energy		DFT/B3LYP SDD	DFT/ B3PW91 6-311G
E_{LUMO}		-1.3031	-1.2838
E_{HOMO}		-5.6092	-5.6895
E_{LUMO+1}		-1.1180	-1.0791
E_{HOMO-1}		-5.9181	-6.0441
Energy Gap	$(\Delta E_{GAP})\lvert E_{HOMO}- E_{LUMO}\rvert$	4.3061	4.4057
Ionization Potential	$(I = -E_{HOMO})$	5.6092	5.6895
Electron Affinity	$(A = -E_{LUMO})$	1.3031	1.2838
Chemical hardness	$(\eta = (I - A)/2)$	2.1530	2.2028
Chemical softness	$(s = 1/2\ \eta)$	1.0765	1.1014
Chemical Potential	$(\mu = -(I + A)/2)$	-3.4561	-3.4866
Electronegativity	$(\chi = (1+ A)/2)$	1. 1515	1.1419
Electrophilicity index	$(\omega = \mu^2/2\ \eta)$	2..7739	2.7593

3.5. Molecular Electrostatic Potential (MEP)

Molecular electrostatic potential energy maps allow us to observe the charge distributions and charged areas of molecules in three dimensions. Understanding charge distributions is essential for determining how molecules interact with one another.[21] It also provides visual information about electronegativity, partial charges, and, dipole moment and the polarity of a structure can be estimated.[22] The MEP map calculated with DFT/B3LYP/SDD and DFT/B3PW91/6-311G methods and basis sets is given in Figure 4. As shown in Figure 4, negative (red or yellow) regions of MEP indicate electrophilic reactivity, while positive (blue) regions represent nucleophilic reactivity.

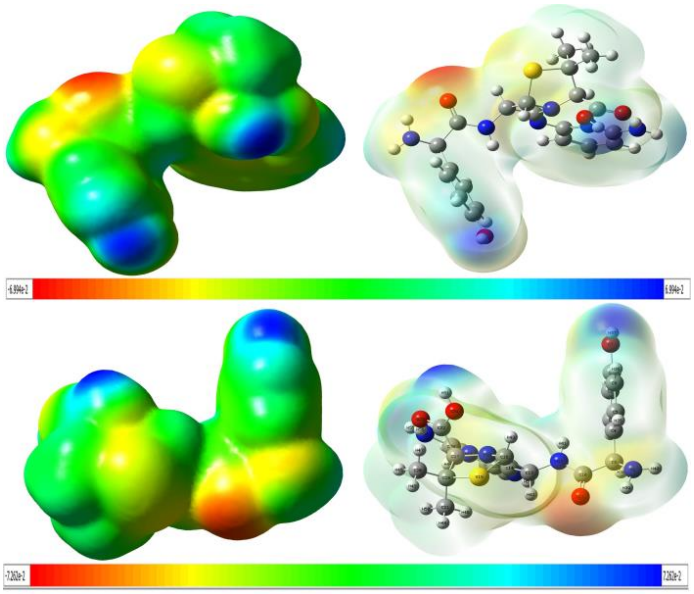

Figure 4. The molecular electrostatic potential surface of the Schiff base complex has been calculated employing the DFT/B3LYP and DFT/RB3PW91 techniques with the SDD and 6-311G basis sets.

DOI: http://dx.doi.org/10.32571/ijct.1410570 E-ISSN: 2602-277X

3.6. Non-Linear Optical Properties (NLO)

In this part of the study, nonlinear properties like dipole moment (μ), molecular polarizability, average polarizability (α), polarizability anisotropy and molecular hyperpolarizability β were calculated for our molecule.[23] The polarizability and hyperpolarizability tensors of the molecule were extracted from the Gaussian output file and their units were translated from atomic unit (a.u.) to electronic unit (esu). for α; 1 a.u.= 0.1482×10^{-24} esu, for β; 1 a.u.= 8.6393×10^{-33} esu).[24] Average polarizability (α), dipole moment (μ) and molecular hyperpolarizability β parameters were obtained with the help of the following equations (1-3).[25] Table 4 shows the hyperpolarization (β), polarization (α), and electric dipole moment (μ), NLO values of the Schiff base compound employing the B3LYP/SDD and B3PW91/6-311G method and basis sets. In order for nonlinear optical (NLO) qualities to be more active, dipole moment, polarizability and hyperpolarizability values must be high. Schiff base compound has a homogeneous charge distribution. For this reason, The molecule lacks a strong dipole moment. The dipole moment was determined as 4.3611 Debye. The highest dipole moment value was determined in the μz (3.3328 Debye) component and the smallest dipole moment value has been determined in the μx (-1.6908 Debye) component. The polarizability and polarizability anisotropy of the Schiff base compound were calculated as $3.60\text{x}10^{-30}$ esu, $3.59\text{x}10^{-30}$ esu, respectively.

$$\mu = (\mu_x^2 + \mu_z^2)^{1/2} \quad (1)$$

$$\alpha = 2^{-1/2}\left[(\alpha_{xx} - \alpha_{yy})^2 + (\alpha_{yy} - \alpha_{zz})^2 + (\alpha_{zz} - \alpha_{xx})^2 + 6\alpha_{xx}{}^2\right]^{1/2} \quad (2)$$

$$\beta = [(\beta xxx + \beta xyy + \beta xzz)^2 + (\beta yyy + \beta yxx + \beta yzz)^2 + (\beta zzz + \beta zxx + \beta zyy)^2]^{\frac{1}{2}} \quad (3)$$

Table 4. The dipole moments (Debye), polarizability (au), components, and total value of Schiff base compound are computed using the SDD and 6-311G basis sets using the DFT/B3LYP and DFT/B3PW91 techniques.

Parameters	B3LYP/ SDD	B3PW91/ 6-311G	Parameters	B3LYP/ SDD	B3PW91/ 6-311G
μ x	-1.6908	-1.6060	β xxx	-5.0538	0.5881
μ y	2.2477	2.2339	β yyy	82.6238	80.6597
μ z	3.3328	3.5437	β zzz	124.3412	123.4437
μ (D)	4.3611	4.4863	β xyy	-121.4026	-111.4193
α xx	-169.2594	-167.6899	β xxy	1.9728	4.2578
α yy	-198.1172	-198.7473	β xxz	41.3306	42.8462
α zz	-181.4276	-182.4134	β xzz	58.6380	56.5629
α xy	-2.6143	-2.8739	β yzz	0.7264	-0.2758
α xz	4.0285	3.7493	β yyz	-13.1721	-10.7833
α yz	-11.9014	-11.2503	β xyz	-29.5064	-29.1733
α (au)	$43.6\text{x}10^{-24}$	$43.5\text{x}10^{-24}$	β (esu)	$3.60\text{x}10^{-30}$	$3.59\text{x}10^{-30}$

3.6. NBO Analysis

In computational chemistry, second-order perturbation analysis of the Fock matrix is utilized to calculate interactions between acceptor (empty)–donor (filled) orbitals in NBO analysis.[26] To understand the delocalization of intermolecular electron density (ED) in the DFT/B3PW91/6-311G basis set of the Schiff base compound, NBO 3.1 program was used together with Gaussian 09W software, and the electron donor (i)), electron acceptor (acceptor (j)) and The E(2) stabilizing energy linked to delocalization was obtained and is given in Table 5.[27] Stabilization energy for the transition between i-j quantum states;

$$E(2) = \Delta Eij = qi\frac{(Fi,j)^2}{(\varepsilon i - \varepsilon j)} \quad (4)$$

Here qi is the donor orbital occupancy rate, εi and εj are the diagonal elements and F(i,j) is the non-diagonal element of the NBO Fock Matrix elements.[28] The strong intramolecular hyperconjugative interaction is seen as a low stabilization energy of 3.39 KJ/mol in the transition from the C3-C4 σ bond to the C2-C3 σ* orbital and 4.52 KJ/mol in the transition from the C5-C6 σ bond to the C1-O7σ* anti-bond orbital. This interaction resulted in 22.59 and 18.83 KJ/mol delocalization to the anti-bonding orbitals of C2-C3 and C4-C5 π^*. The shift from the C25-C26 π^* anti-bonding orbital to the C27-C28 π^* anti-bonding orbital resulted in a relatively substantial stabilization energy of 26.26 kJ/mol. The highest E values are π(C25-C26) /π*(C27-C28) and π(C1-C6) /π*(C4-C5) interactions, respectively.

DOI: http://dx.doi.org/10.32571/ijct.1410570 E-ISSN: 2602-277X

Table 5. Selected NBO results of Schiff base compound are computed using the DFT/B3PW91 technique and 6-311G basis set.

NBO(i)	Type	Occupancies	NBO(j)	Type	Occupancies	E(2)[a] (Kcal/mol)	E (j)-E(i)[b] (a.u.)	F (i, j)[c] (a.u)
C1-C6	π	1.65550	C4-C5	π*	0.36289	22.66	0.30	0.074
C2-C3	σ	1.97351	C3-C4	σ*	0.02486	3.79	1.26	0.062
C2-C3	π	1.69566	C1-C6	π*	0.39852	22.59	0.27	0.072
C2-H33	σ	1.97596	C3-C4	σ*	0.02486	4.21	1.07	0.060
C3-C4	σ	1.97293	C2-C3	σ*	0.01392	3.39	1.27	0.059
C3-H34	σ	1.97818	C4-C5	σ*	0.02680	4.89	1.09	0.065
C4-C5	π	1.65488	C1-C6	π*	0.39852	18.83	0.27	0.064
C4-C8	σ	1.96621	C2-C3	σ*	0.34424	2.56	1.19	0.050
C5-C6	σ	1.97281	C1-O7	σ*	0.02863	4.52	1.00	0.060
C5-H35	σ	1.97610	C3-C4	σ*	0.02486	5.14	1.06	0.066
C8-N9	σ	1.98484	C4-C5	σ*	0.02680	2.19	0.66	0.037
C8-H38	σ	1.95731	C10-O11	π*	0.27738	5.46	0.53	0.051
N12-C13	σ	1.98379	C8-C10	σ*	0.07664	2.55	1.13	0.049
C13-C14	σ	1.95324	N15-C17	σ*	0.04388	7.45	0.95	0.075
C13-C16	σ	1.96325	N15-C17	σ*	0.04388	5.31	0.94	0.063
C14-N32	π	1.98864	C25-C26	π*	0.37494	15.97	0.36	0.072
N15-C17	σ	1.97962	C22-O23	π*	0.22284	1.48	0.74	0.031
N17-C18	σ	1.95418	C22-O23	π*	0.22284	2.26	0.59	0.034
C17-C22	σ	1.97506	C14-N15	σ*	0.07994	2.80	1.07	0.050
C17-S19	σ	1.95269	C21-H50	σ*	0.01371	2.94	0.93	0.047
C20-H47	σ	1.98502	C22-O23	σ*	0.02347	0.67	0.46	0.017
C20-H45	σ	1.98393	C17-C18	σ*	0.05865	5.08	0.81	0.058
C22-O23	π	1.98892	C22-O23	π*	0.22284	0.90	0.37	0.017
C21-H50	σ	1.97742	C18-S19	σ*	0.06363	6.37	0.58	0.055
C25-C26	π	1.63681	C14-N32	π*	0.28065	14.54	0.27	0.057
C25-N32	σ	1.97743	C13-C14	σ*	0.05186	4.69	1.12	0.065
C25-C26	π	1.63681	C27-C28	π*	0.32887	26.26	0.28	0.077
N31-H56	σ	1.98975	C29-N30	σ*	0.49323	4.47	1.18	0.065

3.7. Molecular Docking Studies

Molecular docking is an important step in interpreting biological interactions as well as medication formulation and development. This task is done with the assistance of automated software. To model the molecular recognition process, the molecular docking approach is utilized.[29] This simulation predicts the orientation of a medication relative to a protein in order to generate the most stable combination while reducing the system's energy. Due to its atomic quantum mechanical nature, density functional theory (DFT) is a strong theory. Because of its fascinating accuracy/time ratio in comparison to other quantum approaches, DFT is a particularly essential tool for technological study.[30] The geometry of the synthesized ligand was theoretically studied at DFT levels utilizing Becke's three-parameter hybrid exchange function in conjunction with the Lee-Yang-Parr correlation functional (B3LYP) at 6-311 G(d). AutoDock, Discovery Studio Visualizer, and other databases were used to evaluate and present the findings of molecular docking.[31] Table 6 displays the docking score of Schiff base compound-AChE and Schiff base compound-BChE. The initial stage in the docking procedure is to extract the protein sequences from the protein database as acetylcholinesterase (AChE) crystal structure (PDB ID:6SAM) and butyrylcholinesterase (BChE) crystal structure (PDB ID:6SAM). Some hydrogen bonds are given in Figure 5. Here, the binding mechanism is van der Waals bonded hydrogen VAL-288, PHE-398, SER-198. Water hydrogen bonds are HOH-758 (3.15Å). Hydroxylated LEU-286 (4.65 Å) is DMS-601 (3.47). THR-120 (4.59 Å) is hydrogen bonded to conventional hydrogen bonds. PHE-329 (4.53 Å) and TRP-231 (4.52 Å) bind to the Pi-Alkyl phenyl center. ASP-70 (3.88 Å) Pi-Anion bound to nitrogen. HIS-179 (4.30 Å) binds to the pyrazolone center. GLy-116 (3.32 Å) is bound to nitrogen. Figure 6. A 3D representation of the aromatic surface of the receptor and a 2D view of BChE enzyme interactions are given

Table 6. Docking score of Schiff base compound-AChE and Schiff base compound-BChE

Compound	Docking Score	
	AChE (PDB: 6SAM)	**BChE** (PDB: 4BFT)
Schiff base compound	-6.877	-7.086

DOI: http://dx.doi.org/10.32571/ijct.1410570 **E-ISSN: 2602-277X**

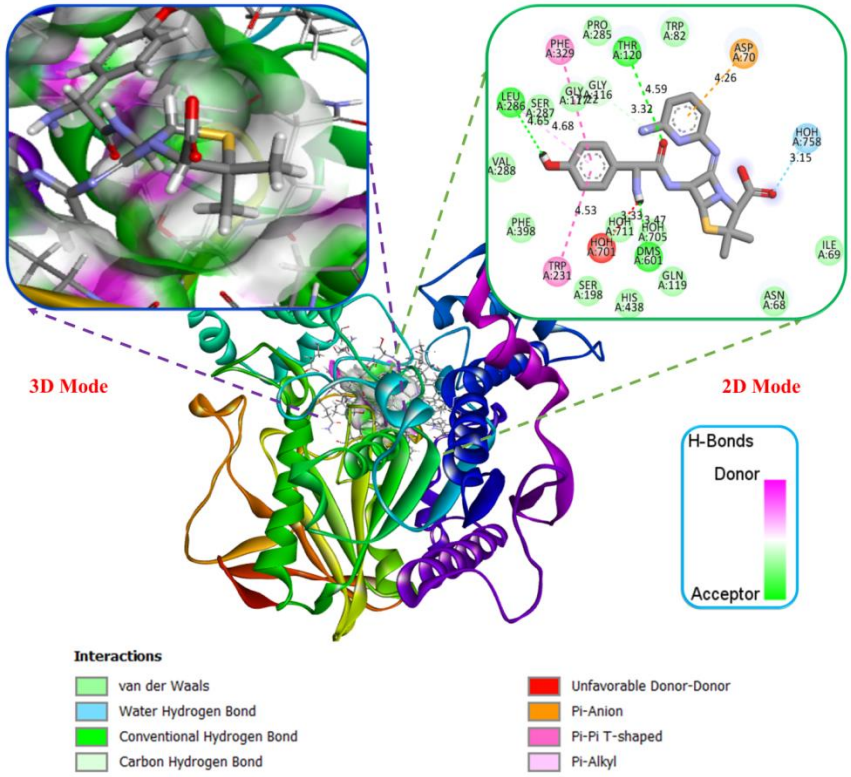

Figure 5. 3D illustration of the aromatic region of the receptor and a 2D picture of the AChE enzyme interactions.

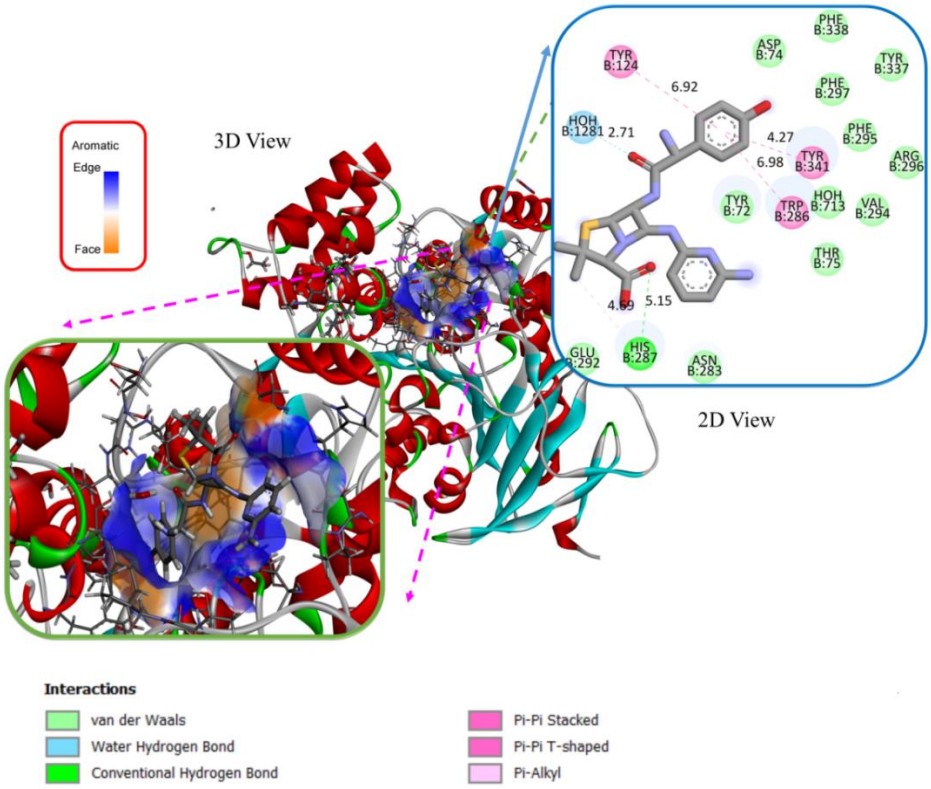

Figure 6. 3D illustration of the aromatic region of the receptor and a 2D picture of the BChE enzyme interactions.

DOI: http://dx.doi.org/10.32571/ijct.1410570 E-ISSN: 2602-277X

4.CONCLUSION

The shape of the optimized molecule was disclosed, as well as its molecular properties, bond length, and bond angle. The Schiff base compound exhibits considerable NLO activity due to its high hyperpolarizability. The Schiff base compound's stability and chemical reactivity were discovered via HOMO-LUMO analysis. The MEP study predicted energy range and the reactive areas of the studied molecule revealed the compound's chemical structure. The NBO approach for calculating stabilization energy has been clarified through both intramolecular and intermolecular events. AChE (shift score; -6.877) and BChE (shift score; -7.086) protein receptors were docked, and the highest and lowest binding energy achieved was -7.086 Kcal/mol with BChE protein. The chemical may exhibit inhibitory effect against AChE and BChE based on molecular splicing data, which might lead to the creation of novel anti-tuberculosis medications. Furthermore, utilizing homology modeling and molecular docking approaches, the biological and medical features of this Schiff base, covering Alzheimer's disease (AD), were investigated. According to the electrophilicity index (13,132), the chemical reactivity analysis revealed a high softness value (0.261 eV) and a low hardness value (1.919 eV); this implies the ligand's strong chemical reactivity and low kinetic stable with considerable intramolecular charge transfer. house). A molecular docking analysis of the interaction between ligand and several cell lines indicates an intriguing binding pattern with proteins, notably those involved in Alzheimer's disease (AD). These chemical reactions occur via many sorts of bonds, including H bonds, van der Waals bonds, conventional hydrogen bonds, carbon hydrogen links, pi-donor hydrogen bonds, and pi-alkyl bonds. They are generated by the nitrogen atoms of the amino and the oxygen atoms of the hydroxyl groups and, azomethine groups, the ligand's lactone and pyrone ring, and the amino acid residues of various receptors. As a result, this ligand can be regarded as a potential contender against Alzheimer's disease (AD).[32]

Conflict of Interest

The authors declare that there is no competing interest.

REFERENCES

1. Hodson, R. *Journa*. **2018**, 559, S1.
2. Soria Lopez, J.A.;González, H.M.;and Léger, G.C., S.T. Dekosky and S. Asthana, Editors. 2019, Elsevier. p. 231-255.
3. Karabulut, B. *Journa*. **2020**, 9(1), 26-35.
4. Ellman, G.L.; Courtney, K.D.; Andres, V.; and Featherstone, R.M. *Journa*. **1961**, 7(2), 88-95.
5. Vijesh, A.M.; Isloor, A.M.; Telkar, S.; Arulmoli, T.; and Fun, H.-K. *Journa*. **2013**, 6(2), 197-204.
6. Al Zoubi, W.; Al-Hamdani, A.A.S.; and Kaseem, M. *Journa*. **2016**, 30(10), 810-817.
7. Shi, L.;Ge, H.-M.; Tan, S.-H.; Li, H.-Q.; Song, Y.-C.; Zhu, H.-L.; and Tan, R.-X. *Journa*. **2007**, 42(4), 558-564.
8. Geddes, A.M.; Klugman, K.P.; and Rolinson, G.N. *Journa*. **2007**, 30, 109-112.
9. Huttner, A.; Bielicki, J.; Clements, M.N.; Frimodt-Møller, N.; Muller, A.E.; Paccaud, J.P.; and Mouton, J.W. *Journa*. **2020**, 26(7), 871-879.
10. Vriend, G. *Journa*. **1990**, 8(1), 52-56.
11. Aihara, J.-i. *Journa*. **1999**, 103(37), 7487-7495.
12. Michael J. Frisch B.S. Gustavo Scuseria, M.R., Richard Cheeseman Jr, Giovanni Scalmani, Barone villagrande, Benedetta Mennucci, *Gaussian 09*. 2009.
13. Karabacak Atay, Ç.; and Ulutürk, M. *Journa*. **2022**, 17(2), 559-567.
14. Sertbakan, T.R. *Journa*. **2021**, 1(2), 46-64.
15. Wiberg, K.B.; and Rablen, P.R. *Journa*. **1993**, 14(12), 1504-1518.
16. Ramalingam, S.; Karabacak, M.; Periandy, S.; Puviarasan, N.; and Tanuja, D. *Journa*. **2012**, 96, 207-220.
17. Jalbout, A.F.; and Fernandez, S. *Journa*. **2002**, 584(1), 169-182.
18. Silvarajoo, S.; Osman, U.M.; Kamarudin, K.H.; Razali, M.H.; Yusoff, H.M.; Bhat, I.U.H.; Rozaini, M.Z.H.; and Juahir, Y. *Journa*. **2020**, 32, 106299.
19. Jeyavijayan, S. *Journa*. **2015**, 136, 890-899.
20. Sevvanthi, S.; Muthu, S.; Aayisha, S.; Ramesh, P.; and Raja, M. *Journa*. **2020**, 30, 100574.
21. Uysal, Ü.D.; Berber, H.; and Aydoğdu Erdönmez, A. *Journa*. **2020**, 24(2), 419-431.
22. Ergan, E. *Journa*. **2021**, 11(3), 2142-2151.
23. Bhuiyan, M.D.H.; Ashraf, M.;Teshome, A.; Gainsford, G.J.; Kay, A.J.; Asselberghs, I.; and Clays, K. *Journa*. **2011**, 89(2), 177-187.
24. Mahmood, A.; Khan, S.U.-D.; Rana, U.A.; Janjua, M.R.S.A.; Tahir, M.H.; Nazar, M.F.; and Song, Y. *Journa*. **2015**, 28(6), 418-422.
25. Thanthiriwatte, K.S.; and Nalin de Silva, K.M. *Journa*. **2002**, 617(1), 169-175.
26. Tanış, E. *Journa*. **2017**, 21(3), 545-563.
27. Padmaja, L.; Vijayakumar, T.; Hubert Joe, I.; Reghunadhan Nair, C.P.; and Jayakumar, V.S. *Journa*. **2006**, 37(12), 1427-1441.
28. Gounden, D.; Nombona, N.; and van Zyl, W.E. *Journa*. **2020**, 420, 213359.
29. Yuriev, E.; and Ramsland, P.A. *Journa*. **2013**, 26(5), 215-239.
30. Kolancilar, H. *Journa*. **2019**, 7(3), 1319-1334.
31. Taherkhani, A.; Orangi, A.; Moradkhani, S.; and Khamverdi, Z. *Journa*. **2021**, 18(1), 16-45.
32. Lane, C.A.; Hardy, J.; and Schott, J.M. *Journa*. **2018**, 25(1), 59-70